Journal Name RSCPublishing

COMMUNICATION

Supporting information: A universal route to improving conjugated macromolecule photostability

H. Santos Silva,[a,b] A. Tournebize,[c,d,e] D. Bégué,*[a] H. Peisert,[c] T. Chassé,[c] J. -L. Gardette,[d,e] S. Thérias,[d,e] A. Rivaton,[d,e] R. C. Hiorns*[f]

[a] Université de Pau et des Pays de l'Adour (UPPA), IPREM (ECP, CNRS-UMR 5254), 2 Avenue Président Angot, 64053 Pau, France.
E-mail: didier.begue@univ-pau.fr
[b] UPPA, IPREM (EPCP, CNRS-UMR 5254), 64053 Pau, France.
[c] Institute for Physical and Theoretical Chemistry, Eberhard-Karls-University, Auf der Morgenstelle 18, D-72076 Tübingen, Germany.
[d] Université Blaise Pascal, Institut de Chimie de Clermont-Ferrand, Equipe Photochimie, BP 10448, F-63000 Clermont-Ferrand, France.
[e] CNRS, UMR 6296, ICCF, Équipe Photochimie, BP 80026, F-63171 Aubière, France.
[f] CNRS, IPREM (EPCP, CNRS-UMR 5254), 64053 Pau, France.
E-mail: roger.hiorns@univ-pau.fr

† The research leading to these results has received funding from European Union Seventh Framework Program (FP7/2011) under grant agreement ESTABLIS no. 290022. Dr. M. Pédeutour is thanked for administrative support.

Contents

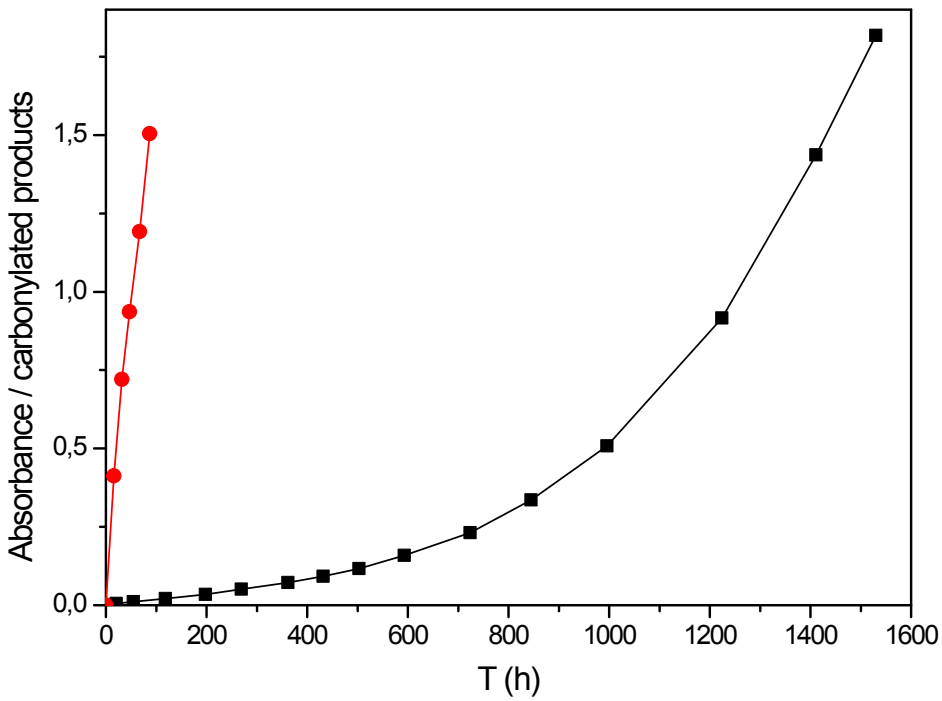

Figure S1. Comparison of the rates of photo-oxidation of polyethylene (PE, black line) and poly(ethylene oxide) (PEO, red line) as indicated by infra-red measurements of the concentration of carbonylated oxidation products.

Note: both films (100 µm) were irradiated in accelerated artificial ageing conditions ($\lambda > 300$ nm, 35 °C). This degradation process is known to be representative of outdoor exposure, see (a) J.-L. Gardette, Fundamental and technical aspects of the photooxidation of polymers, in *Handbook of Polymer Science,* Ed. S. H. Hamid, Marcel Dekker Inc., 2000, 671; (b) B. Ranby, J. F. Rabek, in *Photodegradation, Photooxidation and Photostabilization of Polymers*. Wiley, London, 1975, 493; (c) D. J. Carlsson, A. Garton, D. M. Wiles, *Macromolecules,* 1976, **9**, 695.

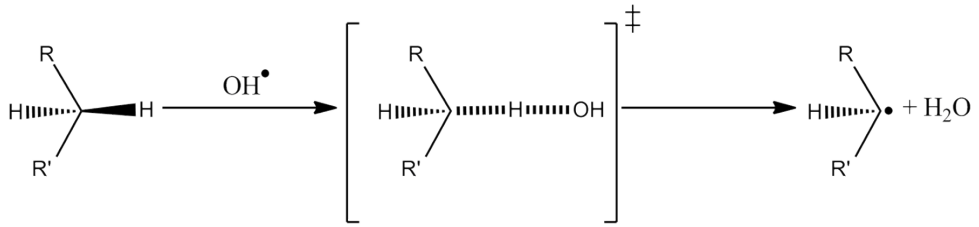

Figure S2. Reaction pathway used to calculate bond dipole moments (BDMs) and bond transition states, consisting of proton abstraction by an $OH^{\bullet}$ radical leading to a transition state, and then carbon-chain radical and water.

Note: we investigated this reaction path by both HF and DFT methodologies in an attempt to access transition states. The dissociation path for these protons upon the abstraction by an $OH^{\bullet}$ radical in **5** and for **6** were calculated using the same systems as those used to calculate E_{BD} values. The maximum of these dissociation curves may indicate a transition state existing between the approaching radical, the abstraction of the proton and the departure of a water molecule leaving behind an unpaired electron on the alkyl chain. The geometries and energies of these states were calculated following a *quasi*-Newton like Hessian mode algorithm. These curves, calculated under several methodologies, can be found in Fig. S3.

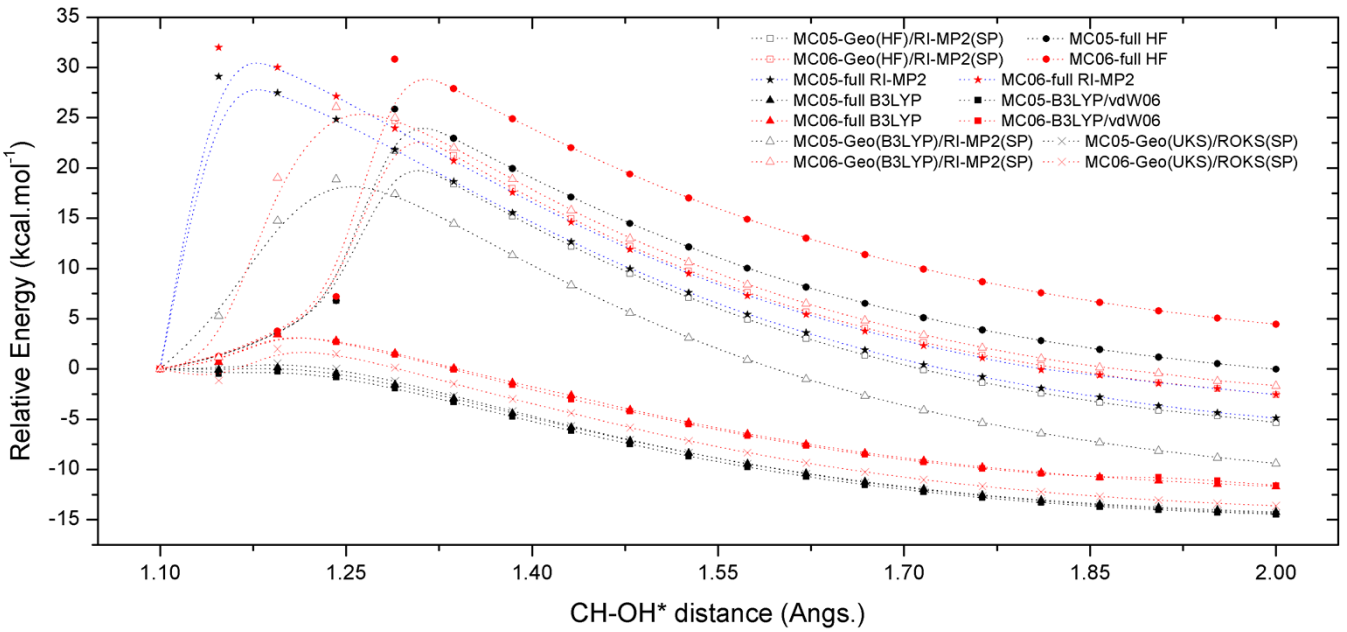

Figure S3. Energetic barrier on the reaction coordinate for hydrogen abstraction by an OH• radical calculated by HF, DFT and RI-MP2 methodologies.

Notes

i) the energy referential was set to a 1.1 Å C-H bond-length in the ground state.

ii) One can observe that DFT methodology cannot access any significant energetic barrier on the internal coordinate system and this "failure" is also observed when attempting to determine an appropriate transition state (also see Fig. S4). The equilibrium distance for the C-H bond is 1.1 Å regardless of the nature of the polymer. At ambient temperature (25 ºC), one has 0.593 kcal mol^{-1} available thermal energy. Thus, one can find a barrier height for the reaction coordinate of 25.8 and 30.8 kcal mol^{-1} for **5** and **6**, respectively. Single point MP2 calculations were performed on the HF geometries and they show the same trend. However, the energy correction introduced by the second order perturbation lowers energetic difference among states from 5 to 3 kcal mol^{-1}. The same calculations were performed for the models **2** and **3**, using the same methodology. The energetic barrier was found, even with the HF-only method, as being reduced by 4.2 kcal mol^{-1}. The scan of the dissociation on the reaction coordinate is presented in Fig. S4.

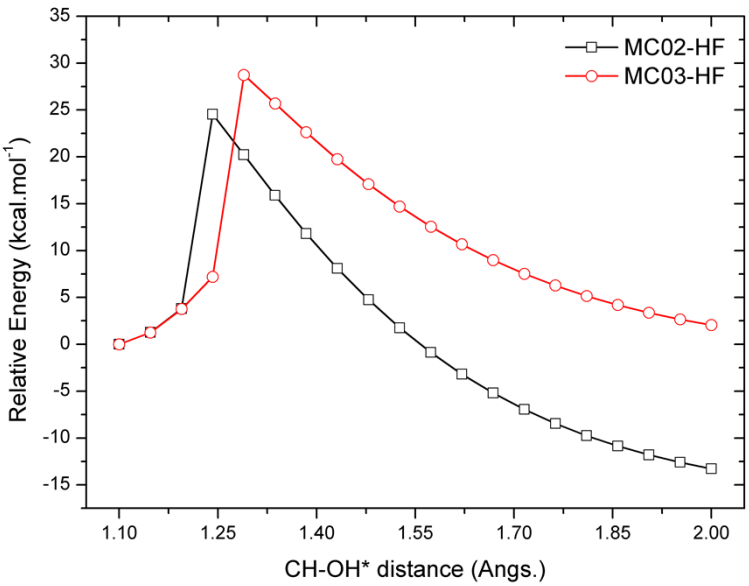

Figure S4. Energetic barrier on the reaction coordinate for the hydrogen abstraction by an OH• radical calculated by HF for **2** and **3**. The energy referential was set to a 1.1 Å C-H bond-length in the ground state.

Note: From the figure, one can deduce that the energetic dissociation barrier is a method-dependent parameter and therefore **cannot** be used as determinant parameter for determination of photostabilities of the studied compounds.

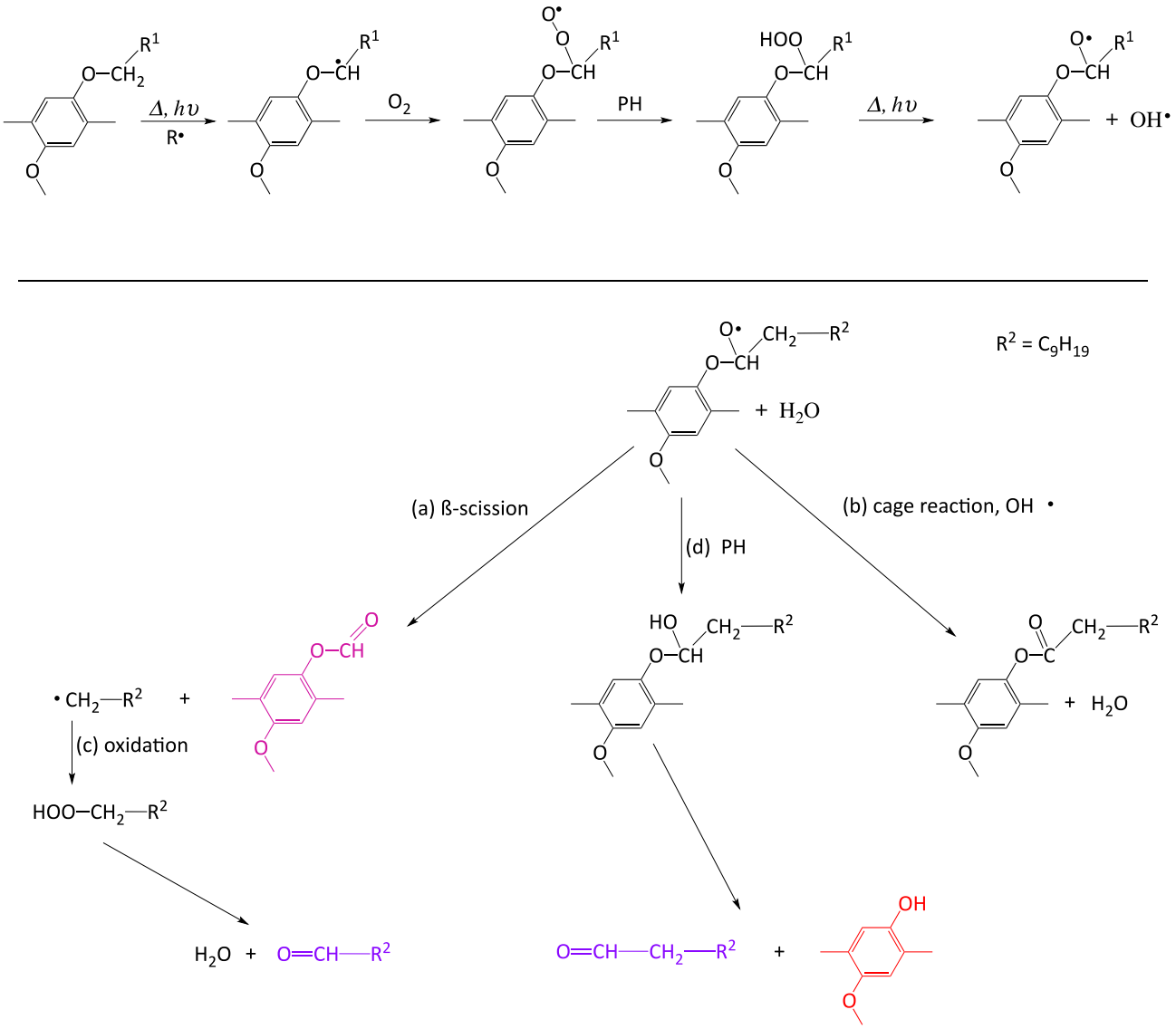

Scheme S1. Proposed chain-radical oxidation of the side-chain of poly[2-methoxy-5-(3',7'-dimethyloctyloxy)-1,4-phenylenevinylene] (MDMO-PPV, also called PH); a possible but no longer considered dominant reaction. Adapted from Chambon, S.; Rivaton, A.; Gardette, J. L.; Firon, M.; Lutsen, L.; *J. Polym. Sci. Pt A: Polym. Chem*., **2007**, *45*(*2*), 317-331.

Note: The photochemical behaviors of poly(phenylenevinylene) (PPV) and its aromatic-oxy-alkyl derivative MDMO-PPV were studied by Chambon *et al*. [Chambon, S.; Rivaton, A.; Gardette, J. L.; Firon, M.; Lutsen, L.; *J. Polym. Sci. Pt A: Polym. Chem*., **2007**, *45*(*2*), 317-331; and Chambon, S.; Rivaton, A.; Gardette, J. L.; Firon, M. *Polym. Degrad. Stab.* **2011**, *96*(*6*), 1149]. It was observed that the absence of an ether substituent ***did not*** increase the rate of photooxidation of MDMO-PPV compared to that of PPV. However, at that time, the sole unambiguous effect of oxygen atom on the photochemical behavior of polymers was studied for aliphatic structures. As shown in Fig. S1, a negative effect was evidenced when comparing PE and PEO and therefore, there was a basic axiom that alkoxy groups resulted in destabilization, even when adjacent to aromatic backbones. Given the understanding that was available in that time, the similarities in degradations of MDMO-PPV and PPV were therefore explained by proposing that PPV structural defects and transient species resulted in its stability being reduced to a level similar to that of MDMO-PPV, a not untoward idea given that PPV remains difficult to prepare given its low solubility. With the results of this current paper, it is no longer necessary to hypothesize on the quality of PPV; the alkyl-oxy-aromatic structure would seem to result in no loss of stability for a given material. In effect, the scheme S1 remains possible, but can no longer be thought dominant.

	Bond Dissociation Energy (kcal mol^{-1})					
Hydrogen	**1**	**2**	**3**	**4**	**5**	**6**
a	85.35	86.17	86.98	88.98	-	-
b		101.36	101.29	101.90	-	-
c		117.46	117.51	117.19	-	-
d		117.46	119.96	116.72	-	-
e		-	-	-	-	-
f	-	92.79	-	-	-	-
g	-	104.74	100.45	98.84	-	-
h	-	-	-	-	104.80	-
i	-	-	-	-	-	101.56

Table S1. Calculated bond dissociation energies (E_{BD}) for model compounds **1-6** within B3LYP/6-31G** level of theory.

	Bond Dissociation Energy (kcal mol^{-1})					
Hydrogen	**1**	**2**	**3**	**4**	**5**	**6**
a	63.03	64.00	59.42	62.61	-	-
b	83.82	83.76	78.23	78.71	-	-
c	102.80	102.24	89.07	96.40	-	-
d	96.91	100.16	85.67	97.05	-	-
e	100.60	-	-	-	-	-
f	-	69.27	-	-	-	-
g	-	85.03	77.65	79.28	-	-
h	-	-	-	-	82.01	-
i	-	-	-	-	-	81.53

Table S2. Calculated bond dissociation energies (E_{BD}) for model compounds **1-6** within HF/6-31G** level of theory.

	Model Compounds Bond Dipole Moments (D)					
Pair Carbon-H_x	**1**	**2**	**3**	**4**	**5**	**6**
C-Ha	0.5338	0.5304	0.5343	0.5328	-	-
C-He	0.5949	-	-	-	-	-
C-Hf	-	0.7945	-	-	-	-
C-Hg	-	0.8154	0.4788	1.0380	-	-
C-Hh	-	-	-	-	0.8347	-
C-Hi	-	-	-	-	-	0.4796

Table S3. Calculated bond dipole moments (BDMs) for model compounds 1-6 in B3LYP/6-31G** level of theory.

Notes:

i) The bond dipole moments $\left|\vec{\mu}\right|_B$ of the pair of bonds C-H_x were calculated using the Löwdin atomic charges with bond distances in the ground state.

ii) The presence of oxygen decreases the value of $\left|\vec{\mu}\right|_B$ regardless of the hybridization of the attached carbon. This is due to the electronegativity of oxygen removing electronic presence at the alpha-carbon, and in turn reducing the BDM on the C-H bond. This effect is also found to happen when oxygen has a mesomeric effect on the conjugated cycle: some partial charge injected comes as well from the attached carbon in the aliphatic chain. One must keep in mind that the polarity of the bond is not a determining parameter for homolytic bond breaking. We have calculated it in order to validate that no trend can be deduced as it is the case of the bond dissociation energies.

	Radical localization probability (%)		
	Native Carbon	**Adjacent oxygen**	**Aromatic ring**
2	39.69	-	12.25
3	59.29	1.44	0.16
5	77.45	-	-
6	59.29	2.25	-

Table S4. Calculated radical localization probability, assumed as the square module of the partition coefficient.